Integration of Laser Scanning and Close-Range Photogrammetry - The Last Decade and Beyond

Beraldin, Jean-Angelo

National Research Council Canada
Institute for Information Technology

Conseil national de recherches Canada
Institut de technologie de l'information

NRC-CNRC

*Integration of Laser Scanning and Close-Range Photogrammetry - The Last Decade and Beyond **

Beraldin, J.-A.
July 2004

* published in the XXth International Society for Photogrammetry and Remote Sensing (ISPRS) Congress. Commission VII, pp. 972-983. Istanbul, Turkey. July 12-23, 2004. NRC 46567.

Canada

INTEGRATION OF LASER SCANNING AND CLOSE-RANGE PHOTOGRAMMETRY – THE LAST DECADE AND BEYOND

J.-Angelo Beraldin [a]

[a] National Research Council Canada, Ottawa, Ont., Canada, K1A0R6 – angelo.beraldin@nrc-cnrc.gc.ca

Commission V, WG V/2

KEY WORDS: Laser Scanning, Close-range photogrammetry, Sensor fusion, 3D sensors, Metric Performance, Heritage, Space

ABSTRACT:

In last decade, we have witnessed an increased number of publications related to systems that combine laser scanning and close-range photogrammetry technologies in order to address the challenges posed by application fields as diverse as industrial, automotive, space exploration and cultural heritage to name a few. The need to integrate those technologies is driven by resolution, accuracy, speed and operational requirements, which can be optimized using general techniques developed in the area of multi-sensor and information fusion theory. This paper addresses an aspect critical to multi-sensor and information fusion, i.e., the estimation of systems uncertainties. The understanding of the basic theory and best practices associated to laser range scanners, digital photogrammetry, processing, modelling are in fact fundamental to fulfilling the requirements listed above in an optimal way. In particular, two categories of applications are covered, i.e., information augmentation and uncertainty management. Results from both space exploration and cultural heritage applications are shown.

1. INTRODUCTION

1.1 Why combine data from multiple sensors?

The topic of multi-sensor data fusion has received over the years a lot of attention by the scientific community for military and non-military applications. Multi-sensor data fusion techniques combine data from multiple sensors and related information from associated databases, to achieve improved accuracies and more specific inferences than could be achieved by the use of a single sensor alone (Hall, 1997). As noted by Hong, 1999, in applying those techniques, one would expect to achieve the following benefits:

- Robust operational performance
- Extended spatial/temporal coverage
- Reduced ambiguity
- Increased confidence
- Improved detection performance
- Enhanced resolution (spatial/temporal)
- Increased dimensionality

To discuss the integration of laser scanning and close-range photogrammetry from a multi-sensor and information fusion point of view, we present the key features of different laser scanner technologies and photogrammetry-based systems that should be considered in order to realize the benefits expected in a multi-sensor platform. Some examples are given to illustrate the techniques. In particular, two categories of applications are covered, i.e., *information augmentation* and *uncertainty management*. As defined by (Hong, 1999), information augmentation refers to a situation where each sensor provides a unique piece of information to an application and fusion extends, for example, the system's spatial/temporal coverage. Uncertainty management is a very important and a critical part of multi-sensor data fusion techniques. It covers situations where different sensors measure the same object/site from different locations or times or even users. In order to deliver the best description of the object/site (lowest uncertainty), one must manage the uncertainties link to the sensing devices, the environment and *a priori* information (e.g. a particular user). The objectives of the data fusion are to minimize the impact of those uncertainties and to get the most out of the multi-sensor platform. In other words, one must justify the increased cost and complexity of a multi-sensor solution.

1.2 Related work

A survey of the literature on multi-sensor data fusion can generate a long list of papers and books describing the theory and the different applications where data fusion is critical. Llinas et al. 1990 describe an application where a moving aircraft is observed by both a pulsed radar (based on radio frequencies) system and an infrared imaging sensor. The pulsed radar system provides an accurate estimate of the aircraft's range but with poor angular direction estimates (due to the longer wavelengths compared to optical light). Instead, the infrared imaging sensor determines only the aircraft's angular direction but with a much higher accuracy when compared to the pulsed radar system. If these two observations are correctly associated, then the combination of the two sensor's data provides an improved determination of location than could be obtained by either of the two independent sensors. This case represents a good example of uncertainty management through an adequate understanding of the sensors error and resolution characteristics.

To model complex environments, those composed of several objects with various characteristics, it is essential to combine data from different sensors and information from different sources. El-Hakim, 2001 discusses the fact that there is no single approach that works for all types of environment and at the same time is fully automated and satisfies the requirements of every application. His approach combines models created from multiple images, single images, and range sensors. He also uses known shapes, CAD drawings, existing maps, survey data, and GPS data.

Surprisingly, some manufactures of lasers scanners discard some information generated by their scanners. All optical three-dimensional (3D) scanners measure the reflectance information generated by the intensity of the returned laser beam but in many cases, the manufacturer eliminates that important information from the raw 3D image file. In an inspection application, El-Hakim et al. 1994 show that the use of intensity data (reflectance) produced by a range camera can improve the accuracy of vision-based 3D measurements. The authors provide a survey (pre-1994) of multi-sensor data fusion methods in the context of computer vision.

Wendt et al. 2002 present an approach for data fusion and simultaneous adjustment of inhomogeneous data intended to increase the accuracy and reliability of surface reconstruction. They aimed at an approach to adjust any kind of data in a combined adjustment and to give adequate weights to each measurement. Their study is based on 3D data obtained from stripe (fringe) projection and photogrammetry-based systems. To validate their approach, they use two types of free-form object surfaces, one being artificial and known is used for test purposes and the other is a tile made of concrete. Johnson et al., 2002 describe a technique for adaptive resolution surface generation from multiple distributed sensors. They demonstrate the technique using 3D data generated by a scanning lidar and a structure from motion system. Other authors compare and discuss practicality issues of laser scanning and digital close range photogrammetry (Velios et al., 2002; CIPA&ISPRS, 2002). Increasingly, laser scanning and photogrammetry are combined for many applications. These applications include documentation of as-built sites like offshore oil and gas structures, process plants, nuclear and power generation stations, architectural and construction sites, industrial manufacturing facilities, automotive production, space exploration and cultural heritage.

In this paper, resolution, uncertainty and accuracy of 3D information measurement in the context of close-range 3D systems are discussed. Laser scanners are reviewed in more details compared to photogrammetry. A number of examples illustrating the importance of sensor characterization are shown. Some comments about the impact of a user in a project are also presented. The goal is not to survey all commercial 3D vision systems or present an exhaustive list of tests of the systems chosen for this paper. Instead, some basic theory about 3D sensing is presented and is accompanied by selected results that should give the reader some pointers in order to become more critical when picking 3D vision systems and a sensor fusion strategy.

2. OPTICAL SENSORS FOR THREE-DIMENSIONAL MEASUREMENTS

In the last twenty years, many advances have been made in the field of solid-state electronics, photonics, computer vision and computer graphics. Non-contact three-dimensional (3D) measurement techniques like those based on structured light and passive stereo are examples of fields that have benefited from all of these developments. In the case of passive techniques (that use ambient light), only visible features with discernable texture gradients like on intensity edges are measured. Active systems and in particular, laser-based systems are used to structure the environment in order to acquire dense range maps from visible surfaces that are rather featureless to the naked eye or a video camera. In order to take full advantage of these vision systems, one must understand not only their advantages but also their limitations. Baltsavias, 1999a compares photogrammetry and airborne laser scanning. This section reviews the basic principles and best practices that underline laser scanners and digital photogrammetry for 3D vision systems in the case of close-range applications. We emphasize laser scanning, as one specific scanner can't be used for volumes of different sizes.

2.1 Laser scanners

Active sensors that use light waves for 3D measurements can be divided into classes according to different characteristics. A number of taxonomies exist in the literature (Nitzan, 1988; Jähne et al., 1999). Here we summarize the main classes and give the practical operating distance camera-to-object:

Triangulation: distance scanner-object about 0.1 cm to 500 cm

- Single spot (1D)
- Profile measurement (2D)
- Area measurement (3D really 2.5D)
  - Galvanometer-based laser scanning
  - Laser probe combined with translation-rotation motors, articulated arms and coordinate measuring machines (CMM), position trackers
  - Multi-point and line projection based on diffraction gratings
  - Fringe and coded pattern projection
  - Moiré effect

Time delay & light coherence

- Time of flight: 100 cm to several km
  - Single point and mirror-based scanning
    - Pulsed lasers
    - AM or FM modulation
  - Full field using micro-channel plates or custom build silicon chips (pulsed or AM).
- Interferometric and Holographic: wide distance range

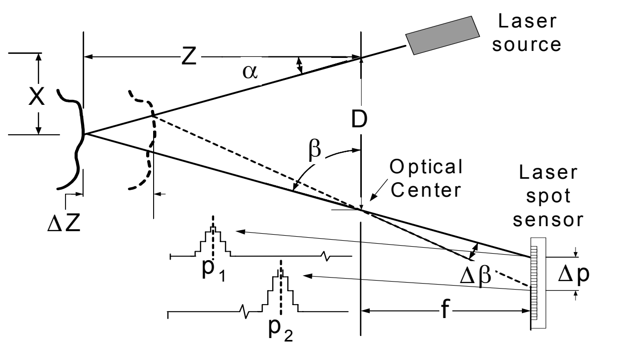

Figure 1. Laser-based optical triangulation (single spot).

2.1.1 Triangulation

Triangles are the basis of many measurement techniques, from basic geodesic measurements performed in ancient Greece to 16th century theodolite-based surveys and now modern laser-based (or projector-based) 3D cameras. The basic geometrical principle of optical triangulation is shown in Figure 1. To acquire a full 3D image, one of the scanning techniques listed above can be used. The collection of the scattered laser light from the surface is done from a vantage point distinct from the projected light beam. This light is focused onto a linear position sensitive detector (herein called laser spot sensor). Knowing two angles (α and β) of a triangle relative to its base (baseline **D**) determines the dimensions of this triangle. The complete range equations are derived in (Blais, 2004).

For an incremental change of distance, **ΔZ**, one measures the incremental angle shift Δβ. This laser spot sensor is in fact an *angle sensor*. The angular shift Δβ caused by the displacement of the surface is observed through a shift in laser spot position **$\Delta p=(p_1 - p_2)$**. For practical matters, the errors with a triangulation-based laser scanner come mainly from the estimate of **p**, through δ_p. An error propagation computation gives the approximation of the uncertainty in **Z,**

$$\delta_z \approx \frac{Z^2}{f\,D}\,\delta_p \tag{1}$$

where f = effective position of laser spot sensor
D = baseline
δ_p = uncertainty in laser spot position
Z = distance to object.

From the equation above, one finds that the measurement uncertainty in ***Z*** is inversely proportional to both the camera baseline and the effective position of the angle sensor wrt the lens, but directly proportional to the square of the distance. Unfortunately, ***f*** and ***D*** cannot be made as large as desired. The baseline ***D*** is limited mainly by the mechanical structure of the optical set-up (stability of the whole system decreases as ***D*** increases) and by shadow effects (self occlusion problems increase with ***D***). Rioux, 1984 presents an approach to triangulation-based range imaging that allows very large fields of view without compromising the performance of the system. The value of δ_p depends on the type of laser spot sensor used, the peak detector algorithm, the signal-to noise ratio (**SNR**) and the imaged laser beam shape. Each sensing method will perform differently (Blais et al., 1986; Naidu et al., 1991). In the case of discrete response laser spot sensors (Beraldin et al., 2003), assuming sub-pixel laser spot position estimation and high **SNR**, the limiting factor will be speckle noise (Baribeau et al., 1991; Dorsch et al., 1994; Jähne et al., 1999; Amann et al., 2001). The effect of speckle noise on spot position uncertainty is approximately given by

$$\delta_p \approx \frac{1}{\sqrt{2\pi}}\,\lambda\,fn \tag{2}$$

where fn = receiving lens f-number
λ = laser wavelength.

For instance, λ=0.68 μm and ***fn***=4, the laser sub-pixel uncertainty is about 1.4 μm. This estimate is for high **SNR** and for well-designed 3D systems. The **SNR** deteriorates rapidly with distance. The fact that the amount of light collected decreases with the distance squared and that the majority of triangulation-based systems don't use optical sensors with a built-in current gain mechanism (like those used in time-of-flight systems) contribute to a deterioration of the SNR. Overall, the maximum range of triangulation-based laser scanners, even with a baseline of 1 m, does not exceed 10 m. A more detailed model of the spatial measurement uncertainty can be derived by computing the actual joint density function of the spatial error (probability distributions). The law of propagation of errors is only an approximation. The complete analysis can show that the spatial error distribution is skewed and oriented with the line of sight, i.e. anisotropic and in-homogeous (Johnson et al., 1997). This is represented schematically on Figure 2.

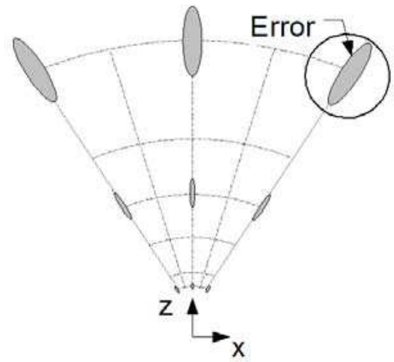

Figure 2. Schematic diagram showing a representation of the shape of the spatial error distribution for a laser scanner.

2.1.2 Time delay systems

A fundamental property of a light wave is its velocity of propagation. In a given medium, light waves travel with a finite and constant velocity. Thus, the measurement of time delays created by light traveling in a medium from a source to a reflective target surface and back to the source (round trip) offers a very convenient way to evaluate distance. The current accepted value for the speed of light in a vacuum is exactly c = 299,792,458 m/sec. If the light waves travel in air then a correction factor equal to the refraction index (depending on the air density) must be applied to c, n ≈ 1.00025 (n-water = 1.33). Let us assume that the speed of light is 3×10^8 m/sec. Different strategies have been devised to exploit this measurement principle: Time-Of-Flight (TOF) with pulsed lasers, Amplitude Modulation (AM), Frequency modulation (FM) systems with or without coherent detection (Koskinen et al., 1991; Baltsavias, E.P. 1999b.; Wehr et al., 1999; Amann et al., 2001).

Long-range sensors (range exceeding 10 m) are usually based on the time-of-flight (TOF) technology (also known as laser radar or lidar for short). The camera to object distance ***Z*** is measured by sending a relatively short impulse of light on a reflective surface and measuring the round trip, **τ**, ***Z*=c*τ/2**. The range uncertainty for a single pulse is approximately given by the following equation:

$$\delta_{r-p} \approx \frac{c}{2}\frac{T_r}{\sqrt{SNR}} \tag{3}$$

where T_r = pulse rise time
δ_{r-p} = uncertainty in range estimation pulse system.

A round trip of **τ**=1 microsecond corresponds to a distance of about 150 m. Assuming a **SNR**=100 and T_r=1 nanosecond, the range uncertainty is close to 1.5 cm. Such a pulse rise time is equivalent to a system bandwidth of about 350 MHz (0.35/1 nanoseconds). Most commercial systems based on TOF provide a range uncertainty in the range 1 cm to 10 cm. Averaging *N* measurements will reduce δ_{r-p} by a factor proportional to square root of *N*. Expansion of the **SNR** can show that the range uncertainty depends on distance and the detection mechanism (avalanche photodiode, etc.). Incidentally, Eq. (3) is similar the result obtain from the estimation of arrival time for the radar ranging problem (Poor, 1994). For high **SNR**, the uncertainty in range estimation is given by

$$\delta_{r-p} \approx \frac{c}{2} \frac{1}{\sqrt{SNR}\ BW} \tag{4}$$

where BW = root-mean-square signal bandwidth.

To lower the range uncertainty, one has to increase the SNR and/or the effective signal bandwidth. This increase in bandwidth agrees with intuition since a large bandwidth corresponds to a signal pulse with sharp edges and hence betters discrimination against background noise. This result for the radar ranging problem can also be applied to peak detector algorithms used in Section 2.1.1. A better estimate of the range uncertainty, $\boldsymbol{\delta_{r\text{-}p}}$, can be obtained by including walk error caused by variations in pulse amplitude and shape (Amann et al., 2001). Finally, TOF systems have an ambiguity interval that is related to the time spacing between consecutive pulses, which can be several kilometres.

Other systems based on continuous wave (CW) modulation get around the measurement of short pulses by modulating the power or the wavelength of the laser beam. For AM, the modulated signal is projected onto a surface, the scattered light is collected on a single photodiode and a circuit measures the phase difference between the two waveforms which in fact is a time delay. The range uncertainty is approximately given by

$$\delta_{r-AM} \approx \frac{1}{4\pi} \frac{\lambda_m}{\sqrt{SNR}} \tag{5}$$

where λ_m = wavelength of the amplitude modulation (c/f_m)
$\delta_{r\text{-}AM}$ = uncertainty in range estimation AM system.

Again, intuition tells us that a low frequency, $\boldsymbol{f_m}$, (long wavelength) makes the phase detection less reliable (see Eqn. 4). Because the returned wave cannot be associated with a specific part of the original signal, it is not possible to derive the absolute distance information from a simple AM method. This is known as the ambiguity interval and can be in the order of several meters. The range ambiguity is given by $\lambda_m/2$. To get around the inconvenience of a range ambiguity interval, one can use multiple frequency waveforms. For instance, assuming a two-tone AM system (low frequency of 10 MHz and high frequency of 150 MHz) and a **SNR**=1000, the range uncertainty is about 0.5 cm (using the high frequency) and the ambiguity, 15 m (using the low frequency). Different papers compare the last two systems (TOF and AM) (Koskinen et al., 1991; Baltsavias, E.P. 1999b.; Wehr et al., 1999).

The last CW system covered in this section is based on frequency modulated (FM) laser radar with coherent detection. Here, the frequency of the laser beam is linearly modulated either directly at the laser diode or with an acousto-optic modulator. The linear modulation is usually shaped by a triangular or saw-tooth wave, which gives rise to what is known as a chirp. The important aspects of this technology are determined by the coherent detection taking place on the optical detector and the fact that the beat frequency resulting from this optical mixing encodes the round trip time delay using a much smaller bandwidth compared to TOF systems (Amann et al., 2001; Schneider et al., 2001). It can also determine absolute distances. These systems can achieve for a tuning range of 250 GHz, a measurement uncertainty of about 10 μm (Schneider et al., 2001). For instance, some commercial systems can provide, over a range of 2 m to 10 m, a measurement uncertainty of about 40 μm at a data rate of 10 points/sec and 150 μm at about 1000 points/sec. Furthermore, the dynamic range is about 10^9. Interesting enough, for ranges between 2 m and 10 m, there is a limited number of laser scanners available commercially. In fact, this range of distances represents a transition between triangulation and time delay-based systems. Triangulation-based systems require a large baseline to operate in that range. On the other hand, time-delay systems can achieve relatively low measurement uncertainty in that distance range but have to face other concerns like higher costs and in some cases limited operating depth of field (Blais, 2004). Furthermore, because of the increased distance attainable with time delay-based systems, the scanning mechanism can produce non-negligible errors. For example, a galvanometer-based scanner with an angular uncertainty of 50 μRad produces at a distance of 200 m a lateral spatial uncertainty of about 1 cm (in a direction perpendicular to the laser beam, see Figure 2). This fact cannot be neglected at long distances especially when the scanner manufacturer uses a laser with low divergence.

2.2 Close-range digital photogrammetry

In this section, we won't go in the details of photogrammetry. It is a topic that is well covered by the ISPRS society's conferences. The variety of techniques available and level of expertise is such that 3D reconstructions and feature measurements are done on heterogeneous sources of images. For instance, Gruen et al. 2003 report the results of their photogrammetric work on the Great Buddha of Bamiyan. The authors performed a computer reconstruction of the statue, which served as basis for a physical miniature replica. The three-dimensional model was reconstructed from low-resolution images found on the Internet, a set of high-resolution metric photographs taken in 1970, and, a data set consisting of some tourist quality images acquired between 1965 and 1969.

We now look at some issues and best practices that are important when integrating this technology with 3D laser scanners. The latest shift in photogrammetry has been the passage to fully digital technologies. In particular, low cost digital cameras with high pixel counts (> 6 mega-pixels image sensors), powerful personal computers and photogrammetric software are driving a lot of new applications for this technology. The fundamental principle used by photogrammetry is in fact triangulation, which is illustrated on Figure 1 for laser scanners. By replacing the projector by another camera, one gets a two-camera arrangement (also called stereoscopy). In its simplest form, a feature is observed from two distinct views and the two corresponding lines of sight are intersected in space to find a three-dimensional coordinate (forward intersection). In actual situations where the measuring chain is not perfect (poor image contrast, noise, etc.), a multi-station convergent geometry must be used in a bundle adjustment in order to minimize the three-dimensional coordinates uncertainties.

The range equations are expressed in terms of camera baseline, distance (camera-object) and the so-called stereo disparity. Usually the baseline to depth ratio (**D/Z**) is used to characterise a given set-up. Errors in detecting the centroid of a particular target on the image sensor of the stereoscopic system produce errors in determining the location of the target in object space.

Similar to laser range scanners, the uncertainty is not a pure scalar function of distance to the target. A more complete camera model and exhaustive error representation can show that the error distribution is also skewed and oriented with the line of sight like laser scanners (see Figure 2). Nevertheless, to get lower uncertainty one needs geometric configurations (large baseline, shorter distance camera-target), a long focal length (not always possible), a low disparity measurement uncertainty and multiple images (in a multi-station convergent geometry). Camera model is covered by Atkinson, 1996. This reference gives the details of the collinearity equations for the three-dimensional case where both internal (focal length, scaling, distortions) and external (pose matrix containing both rotation and translation information of a camera) parameters of a multi-camera arrangement are considered. The complete system of equations can be solved by the bundle adjustment method. If the interior parameters are not available prior to this step (through an adequate camera calibration), a self-calibrating bundle adjustment is used. Actual lenses have optical aberrations. Of these aberrations (spherical, coma, etc.), only optical distortions are modelled in photogrammetry. Calibration of the internal parameters of a camera is critical for accurate measurements. Self-calibration is necessary if camera settings are unknown and vary between images. But to achieve accurate self-calibration, certain geometric configurations of images are needed. Since this is not guaranteed at the project site, and makes imaging more restrictive, it is sensible to decide on high-quality camera and take the images at fixed known settings. Many modern digital cameras can save a number of settings. We then calibrate in the lab at those settings using surveyed points. Figure 3 shows an example of an array of targets arranged on two walls that provide a 3D grid for camera calibration.

Figure 3 Calibration targets placed on walls.

Fraser, 1987; Forstner, 1994; El-Hakim et al., 2003 discuss the need for accuracy evaluation tools for 3D image-based modelling and identify the key factors and critical configurations affecting this accuracy. Since internal evaluation using the covariance matrix may give too optimistic results (particularly for weak geometry, low redundancy, and presence of systematic errors), El-Hakim et al., 2003 propose a novel technique that creates simulated data based on the actual project data. The simulation was very useful in uncovering behaviour that the covariance matrix alone did not reveal. As a result, guidelines for some phases of 3D modelling from images are given. They focus on modelling relatively large structures like monuments and architectures for accurate documentation where knowledge of uncertainty is important. Here are the most significant conclusions:

• In practice, it is difficult to achieve optimum network design. Therefore, the goal should be to avoid weak geometric configurations, low redundancy, and incorrect calibration.

• To avoid low redundancy, points should be tracked over 4 or more images, at least two of which have baseline to depth ratio of 0.4 or larger, and over at least 6 images for closely spaced sequences. This is the most effective way to increase accuracy even for poor configurations.

• Weak geometric configurations are directly function of the baseline to depth ratio, and the effect is more pronounced when this ratio is small (**D/Z** is less than 0.3).

• Since conditions for accurate self-calibration may not be achievable in practice, separate camera calibration at the focal settings used in the actual project is recommended.

• On natural features, the accuracy of the input data improves significantly as camera resolution increases, while the improvement is less significant on well-defined large resolved targets.

• In practical projects, using natural features and less than optimum configuration, but high redundancy and correct pre-calibration, we can expect about 1: 4000 to 1: 10000 accuracy. This should be reduced if practical conditions reduce the redundancy or the pointing precision.

It is interesting to note that a 2D camera can address problems in a wide range of volumes. This is not the case for laser scanners as demonstrated in Section 2.1!

3. CHARACTERIZATION OF 3D SYSTEMS

3.1 Signal detection chain

Beyond the 3D sensing technique used (see Section 2), the measurement of shape, appearance and motion parameters of an object using optical techniques depend on the characteristics of the different elements found in the measuring chain:

- Sensor detection modes: incoherent versus coherent, current gain mechanism with Avalanche Photodiodes (APD) or Micro-channel Plates (MCP)
- Light source spatial considerations: extended, point, line, grid, random patterns, coded pattern projection, scanned or not
- Operating wavelength: single/broad spectrum, visible
- Temporal considerations: AM or FM modulated, pulsed
- Power versus dwell time (data rate) on target object

Furthermore, we should add the following system level aspects:

- Object modification: retro-targets, paint, abrasion
- Object type: topology, material, size
- Level of development: prototype, commercial
- System location: laboratory, shop floor, remote site
- User levels: novice, skilled, expert

Combination of the above listed elements and aspects will determine the final system characteristics:

- Dimensionality: field-of-view (FOV), depth-of-field (DOF), standoff, maximum range
- Spatial discrimination: resolution, uncertainty and accuracy
- Costs to: purchase, use, repair and calibrate

We now cover some of these characteristics in the following sections.

3.2 Spatial discrimination

3.2.1 Laser beam propagation & resolution

Optical laser scanners resolution is limited by the diffraction of the laser light. Calculating the maximum possible spatial resolution requires an arbitrary definition of what is meant by resolving two distinct features. The Rayleigh Criterion assumes that two points sources can be assumed as being separate (resolved) when the centre of the Airy Disc (imaged) from one overlaps the first dark ring in the diffraction pattern of the second. Even in the best emitting conditions (single mode), the laser light does not maintain collimation with distance (e.g. check the beam divergence on scanner specifications sheets). In fact, the smaller the laser beam, the larger is the divergence produced by diffraction. For most laser scanning imaging device, the 3D sampling properties can be estimated using the Gaussian beam propagation formula and the Rayleigh criterion. This is computed at a particular operating distance, wavelength and desired spot size within the volume. Figure 4 illustrates that constraint (λ = 0.633 µm). The solid line shows the relationship between the X and Y axes (direction perpendicular to the laser projection) and the physical dimensions of the object to be scanned. A detailed analysis of this propagation property as applied to 3D scanners can be found in (Rioux et al., 1987; Beraldin et al., 1994). A number of scanner manufacturers use laser re-focusing techniques to achieve better resolutions at a cost of slowing down the effective acquisition data rate.

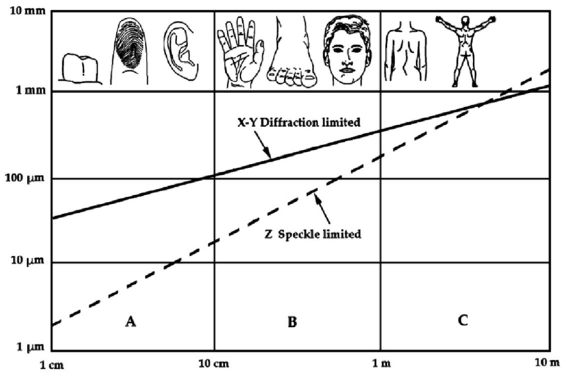

Figure 4. Physical limits of 3D laser scanners as a function of volume measured. Solid line: X-Y spatial resolution limited by diffraction, Dashed line: Z uncertainty for triangulation-based systems limited by speckle, from Rioux 1994.

For 2D cameras used in photogrammetry and texture mapping applications (see Section 4.3), one must match the sensor pixel size to how well an image can be resolved within an adequate depth of field (**DOF**). In these imaging applications, spatial resolution can be limited by diffraction. The smallest resolvable feature, d, for a circular aperture is given by

$$d \approx 1.22\,\lambda\,fn \tag{6}$$

where d = smallest resolvable feature
λ = light wavelength (e.g. 0.55 µm)
fn = lens f-number (e.g. f/22, f/4, etc.)

For example, at 0.55 µm and for **f/8**, the smallest resolvable feature is about 5.4 µm (close to typical pixel sizes). Another example of interest (for display systems) shows that for the human eye with a pupil diameter of about 2 mm (bright room) can resolve 1 arc-min or for **f**=20 mm, 6.7 µm (matches the eye receptors). Finally, the **DOF** for an imaging system is approximately given by

$$DOF \approx \frac{Z^2}{f\,\Phi} Blur \tag{7}$$

where Z = distance lens-object
Blur = blur spot (circle of least confusion)
Φ = aperture diameter

For example, at **Z**=2.5 m, **f**=25 mm, **Blur spot** ≈ 5.5 µm and **Φ**=1 mm (**f/22**), than the depth of field is about 1.4 m. Some camera systems use the Scheimpflug condition to extend the system's DOF (see Beraldin et al., 1994 for laser scanner case).

3.2.2 Measurement uncertainty

As described above, diffraction limits impose a constraint on the resolving power along the **X** and **Y**-axes. For laser triangulation systems, along the range axis (**Z**), one could expect a continuous improvement as the amount of laser power is increased. Unfortunately, this is not the case; indeed the coherence of the laser light produces damaging interference effects known as speckle noise which limits the resolving power of the laser spot sensing (see Section 2.1.1). When the uncertainty due to speckle (**δp**) is projected back into the scene (**δz** – see eqn.(1)), it often means hundreds of micrometers in triangulation-based system (doted line in Figure 4).

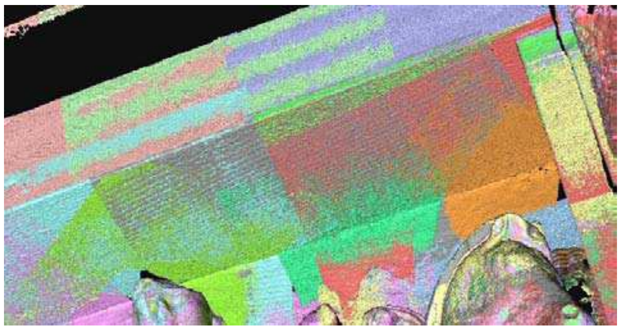

Figure 5. Wave (undulations) phenomenon created by the motion of the 3D camera wrt the scene.

We discussed uncertainty, which represents the random part of the total system errors. The other part is the systematic error. All 3D systems exhibit this type of error to different degrees and for different reasons (e.g. poor calibration). Waves in the raw 3D images are produced when the camera or the object being scanned moves. This is shown in Figure 5. The waves can be removed by proper sensor choice (faster scanner), reducing motion or filtering the raw 3D images. Unfortunately, filtering can altar the spatial resolution.

3.3 Objects material and surface texture effects

It is said that with structured light (active) approaches, minimal operator assistance is required to generate a large quantity of 3D coordinates, and that the 3D information becomes relatively insensitive to background illumination and surface texture. The first comment is indeed true if you compare to methods based on contact probes or photogrammetry. But one must be aware that not all the 3D information is reliable (Soucy et al., 1990; Paakkari, 1992; Hebert et al., 1992; El-Hakim 1994,1995; Boehler et al., 2003). The latter comment about surface texture is somewhat true as long as proper focusing and image processing techniques are used wisely (Soucy et al., 1990). Nonetheless, one should remember that the underlying hypothesis of active optical geometric measurements is that the imaged surface is opaque and diffusely reflecting. Hence, not all materials can be measured accurately like vapour-blasted aluminium (VBAl). Problems arise when trying to measure glass, plastics, machined metals, or marble (see Figure 6). As reported by Godin et al. 2001, marble departs from this hypothesis, and exhibits two important optical properties in this context: translucency, and non-homogeneity at the scale of the measurement process.

Figure 6. Laser spot projected on a marble surface.

This structure generates two key effects on the geometric measurement: a bias in the distance measurement, as well as an increase in noise level, when compared to measuring a reference opaque surface like VBAl. They show results for triangulation-based laser scanners. With their system, they estimated the bias to be about 25-30 µm and the range uncertainty rises from 10 µm on VBAl to 25-50 µm according to the spot size (as with many similar commercial systems).

In another experiment, a flat piece of VBAl and a marble area on a pedestal were measured conducted using both a FMCW system (see Section 2.1.2) and a triangulation laser scanner (see Section 2.1.1),. In both cases, a plane equation was fitted using the same algorithm. The FMCW system gave 14 µm on VBAl and on marble, 87.6 µm (both at a distance of 4 m). The laser triangulation system gave 30 µm on VBAl and on marble, 49 µm (at a distance 30 cm). This last system follows the results presented in Godin et al., 2001. The FMCW behaved in a surprising way! Additionally, the type of feature being measured is an important factor affecting the accuracy of a machine vision system. The accuracy of active 3D cameras drop when measurements are performed on objects with sharp discontinuities such as edges, holes, and targets (Soucy et al., 1990; Wallace et al., 1999; Boehler et al., 2003). This means that systems based on only range will not provide sufficient data for these applications (El-Hakim et al., 1994). The following is a list of concerns encountered with laser scanners (and 3D vision system in general):

- Occlusions/Shadows
- Abrupt texture and shape variations: Edge curl (Buzinski et al., 1992)
- Laser finite footprint and spread on sloped surfaces
- Specular reflections (Fisher et al. 1993)
- Motion: scene, object, ambient vibrations

Therefore, selecting a vision system for a particular application must take into account the ability of the system to measure the features of interest with the required accuracy. Many applications (like found in cultural heritage) do not allow any alterations to the object to suit the vision system, e.g., by placing markers or changing the reflectivity of the surface.

3.4 Calibration and standards

A measurement result has only a meaning if its uncertainty is known no matter if it is large or small compared to others. Here we give a famous quotation taken from Lord Kelvin: "*When you can measure what you are speaking about, and express it in numbers, you know something about it; but when you cannot measure it, when you cannot express it in numbers, your knowledge of it is of a meagre and unsatisfactory kind: it may be the beginning of knowledge, but you have scarcely, in your thoughts, advanced it to the stage of science.*" - Sir William Thompson, Lord Kelvin (1824-1907). It should summarize the importance of knowing how a 3D system measures physical quantities.

The statement of uncertainty is usually based on comparisons with standards traceable to the national units (SI units). For example, standards are available to manufacturers of theodolites and CMMs for assessing their measuring systems. A guideline called VDI/VDE 2634 has been prepared in Germany for particular optical 3D vision systems. It contains acceptance testing and monitoring procedures useful for evaluating the accuracy of optical 3D measuring systems based on area scanning. The guideline applies to optical 3D measuring systems, which works according to the principle of triangulation, e.g. fringe projection, moiré techniques and photogrammetric/scanning systems. Though no internationally recognised standard or certification method exists to evaluate the accuracy, the resolution, the repeatability, the measurement uncertainty of laser range cameras, the user should devise techniques to ensure a confidence level on what is being measured. Definitions of terms can be found in the VIM standard for metrology (VIM 1993). The user should still perform periodic verifications even if the manufacturer provides a specification sheet. Studying scientific literature published on testing range cameras and attending conferences like this one should help in preparing a verification methodology that best suit the user's needs. Boehler et al. 2003 and Johansson 2002 present detailed experimental results on different laser scanners.

In practice, an object that is distinct from the calibration equipment and for which the accuracy is ten times better than that of the range camera will be employed in such an evaluation. A laboratory can be dedicated to calibration and evaluation of machine vision sensors and systems. The main objectives could be

- to perform precise calibration of various types of sensors and systems,
- to monitor sensor stability over time and under variations in environmental conditions such as temperature and ambient light,
- to evaluate system geometric measurement accuracy on a wide range of specially designed standard objects and high-precision positioning devices, and,
- to validate computer vision algorithms, such as target and edge measurement, multi-view registration, model-based recognition, and sensor fusion.

Unfortunately, it is not always possible to own and maintain such a facility. Furthermore, bringing a verification object (especially if it has to be accurate) to a remote site could be difficult.

4. PROCESSING, MODELLING & TEXTURE

Processing can be summarized in the following broad categories: scanner acquisition, 3D modelling with or without texture mapping (Soucy et al. 1996 present a description of the complete processing pipeline: align, merge, edit, compress), geo-referencing, inspection/verification (lengths, angles, radii, volumes, barycentre) Callieri et al., 2004; Beraldin et al., 1997, CAD drawings (cross-sections, pipe center line) and transformation into derived products (VR representations, ortho-photo). This list can be expanded further but we will restrict our discussion to a few examples.

4.1 Scanner acquisition

As an example, two scans were performed on a mostly specular surface (bronze) see Figure 7a. The scanner software used could estimate the surface shape but it did not flag the user that the uncertainty and spatial resolution were off target or that saturation occurred in the 3D image (Figure 7b). The user is left with the time consuming task of deciding to proceed with a low-resolution 3D scan or remove manually the saturated zone (Figure 7c). This situation is typical of interface software supplied with scanners. User intervention becomes critical in order to achieve the quality goals stated for a project. For a novice user, this situation can become quite challenging not to mention costly in terms of time and money.

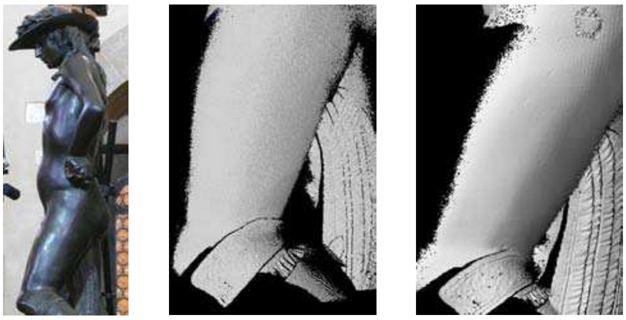

a) b) c)

Figure 7. Scanning on a highly reflective surface with a triangulation-based system, a) bronze sculpture of David by Donatello, b) low resolution scan performed at 30 cm standoff, c) scan at a closer distance, 15 cm, showing better resolution but saturation zone (upper right corner on thigh).

4.2 Model building

Like in many fields of endeavour, expertise is hard to acquire. Three-dimensional acquisition and modelling and certainly, 3D inspection do not escape from this fact. We can distinguish three main classes of users, i.e. novice, skilled and expect. There is no standard in this field defining these classes. The world of CMM has a way to do just this, for 3D, well, maybe in the future. Figure 8 shows an example taken from a project on which we are currently working. We are re-creating Temple C of Selinunte in Sicily using a suite of technologies and expertise (scientific, technical and historical). In one of the task, a Metope was scanned and the 3D modelling was performed by two different users, one that we consider skilled and the other, an expert. Figure 8a) shows the result after alignment, merging and compression in the case of the skilled user. This mesh representation contains about 18 000 polygons. The expert user produced the result shown in Figure 8b) starting from the same 3D images and the same software package. This mesh contains only 10 000 polygons. From this simple experience, one might be tempted to conclude that the scanner could be of low resolution or the modelling software is of poor quality (or both). It is only through a proper understanding of the complete measuring and processing chain (user included) that one can take full advantage of seemingly different but complementary technologies. It is interesting to note that many authors are now including 3D cameras error models in the processing pipeline. For instance, Okatani et al., 2002 developed a method for fine registration of multiple view range images considering the camera measurement error properties. Johnson et al., 2002 describe a technique for adaptive resolution surface generation based on probabilistic 3D fusion from multiple sensors.

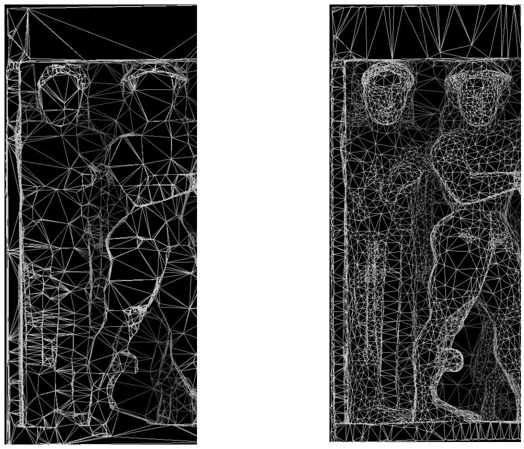

a) b)

Figure 8. 3D modelling and compression as a function of user skills. Same data and modelling software (the figures are not inverted!), a) 18 000-polygon model prepared by a skilled user, b) 10 000-polygon model prepared by an expert user.

4.3 Appearance modelling and visual acuity

Appearance modeling includes methods like image perspective techniques (IPT) and reflectance modelling. The true appearance of an object is the result of the interaction of light with material. Many mathematical models to describe this phenomenon have been proposed in the literature. The knowledge of such a model is important in order to reproduce hypothetical lighting conditions under varying observation points. Techniques that map real-scene images onto the geometric model, also known as IPT have gained a lot of interest. High-resolution colour images can be precisely mapped onto the geometric model provided that the camera position and orientation are known in the coordinate system of the geometric model. The main challenges are computing accurately lens distortions, estimating 2D camera to 3D-model pose, dealing with hidden surfaces, incomplete views and poor lighting condition for external scenes.

In choosing the level of details required for a VR representation, one can consider the following approaches when measuring objects and sites: use instruments that can record details according to some 3D sampling criterion, use instruments to their best performance even though the surface details can't all be captured and present the results by taking into account the human visual system. Using the design equations of Section 3.2, one can prepare a VR show that optimizes the information content from heterogeneous sources: 2D texture from cameras, 3D model quality (resolution + uncertainty), system constraints and human visual acuity.

5. APPLICATIONS

Cultural heritage and space exploration applications are presented in this section. Both information augmentation and uncertainty management examples are covered.

5.1 Information augmentation

The Abbey of Pomposa is one of the most appealing Italian churches of the Romanesque period. It is a complex made of several architecturally simple buildings with mostly planar surfaces. There are also three arches decorated with brick and stonework. The main façade is ornamented with several bas-relief works of art. Except for those, all the structures have been completely modeled using a 4 mega-pixel digital camera. Seven different sets of images were acquired including one from low altitude airplane and one inside the entrance hall of the church (in 2002). The resulting seven models are shown in Figure 9a. Details like the left wheel and the peacock carvings (Figure 9b) were scanned with our Biris 3D sensor in 1998. The level of details of the scanned sections, which was acquired at 0.5 mm resolution, is much higher than the other regions. It is more convincing when viewing these sections up close while navigating through the model. We import points from the detailed model (wheel, peacock) along the perimeter of common surfaces into the less-detailed model. Then we adjust the latter's mesh with the new added points to create a hole into which we insert the detailed model without overlaps. Finally, points from adjacent models on the borders of the gap are used to re-triangulate it so that we have realistic surfaces rather than perfect planes in the filled gap (El-Hakim et al., 2003).

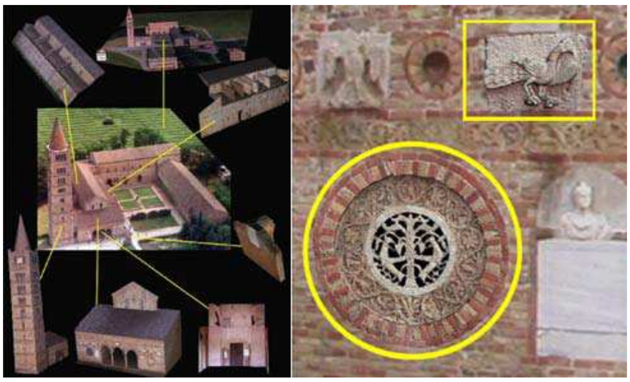

a) b)

Figure 9. Elements used to build the 3D model of the Abbey.

The goal of this project is to show different methods available to model a site for visualization, documentation, preservation and remote fruition. Snap shots, one shaded and one textured, from the complete model are shown in Figure 10.

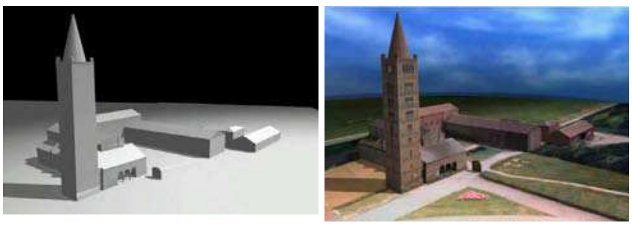

Figure 10. Complete site, a) shaded view of 3D model, b) texture mapped model.

5.2 Uncertainty management

5.2.1 Case 1: Cultural Heritage

In spite of the detailed information produced by 3D optical technologies, in some cases, the method for generating a digital model from multiple 3D acquisitions involves the propagation of errors. These errors limit the overall metric accuracy attainable with such procedure (Jokinen et al., 1998; Okatani et al., 2002). The uncertainty in the alignment of 3D images (pose estimation) depends among other things on the range uncertainty, the size of the overlapping region between 3D images and the curvature of the object surface (Laboureux et al., 2001). For instance, propagation of errors occur when a 3D scanner can only produce the targeted spatial resolution and range uncertainty within a relatively small field of view (single 3D image) compared to the overall size of the object or site being surveyed. The other troublesome situation presents itself when the single 3D image has the required specifications within a large field of view but the object or site contains unacceptable 3D (and texture) features that don't allow proper locking of the 3D images between themselves (flat walls, object can't be closed, presence of range artefacts, etc.). A procedure by which the metric reliability of the 3D model can be assessed and guaranteed to an acceptable level is necessary. Some commercial systems are available on the market, which combine a 3D scanner and a photogrammetric solution (Colet, 2003). Unfortunately, very little information in the literature is available to a wider public interested in knowing the details of the procedure (Scaioni et al., 1996). Guidi et al., 2004 present a method aimed at the verification and correction of the accuracy of a 3D model of a wooden sculpture obtained through iterative alignments of about 170 single 3D images. Though 3D data was acquired with a fringe projection system, the same method can be used with a laser scanner. Figure 11 shows schematically the process where non-impeding optical targets were specifically designed for placement around an object like a sculpture. These targets are measured using a close range digital photogrammetry technique and a 3D scanner. From these measurements, transformation matrices are calculated. Each matrix allows for the pose calculation of the key 3D images from the local coordinate system of the range camera to an accurate global coordinate system determined by the digital photogrammetric procedure. These key 3D images are locked in place and the alignment of the other 3D images proceeds normally. For that sculpture (overall dimension of some 180 cm), the results show a maximum vertical deviation of below 0.5 mm. Close to an order of magnitude improvement was achieved. A metric camera was also used for comparison.

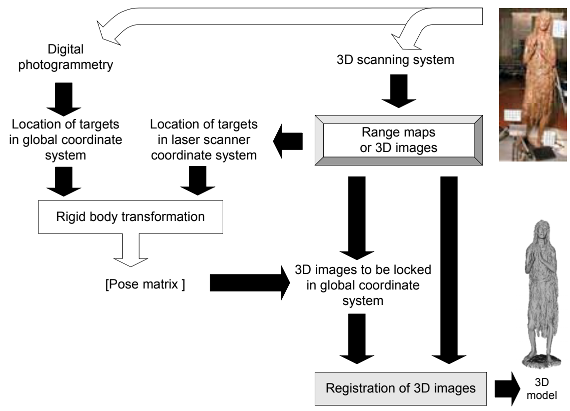

Figure 11. Example of processing steps and data flow for the integration of photogrammetry and 3D scanning systems (adapted from Guidi et al., 2004).

5.2.2 Case 2: Space Exploration

Canada plays an important role in the Space Program and the National Research Council of Canada (NRCC) has been a key player in Canada's contribution to the space initiatives. A key technology is the Space Vision System (SVS) used on-board the Space Shuttle. It tracks the small black dot targets visible in Figure 12. Because the locations of these features on the object are known, object position is computed from their relative positions in the video images using spatial resection. Accuracy and ruggedness to harsh lighting conditions (sun illumination and earth albedo) and environments became important issues during several missions.

Figure 12. The existing Space Vision System uses the known locations of the B/W targets to compute the pose of objects (Photo reproduced with permission from NASA).

In the summer of 1999, an NRCC built laser scanner prototype (triangulation) addressing those issues was successfully interfaced to the current SVS. The scanner uses two high-speed galvanometers and a collimated laser beam to address individual targets on an object. Very high resolution and excellent tracking accuracy are obtained using Lissajous scanning patterns (as opposed to raster scanning). Laser wavelengths at 1.5 μm (eye-safe), 0.82 μm (infrared), and 0.523 μm (green) have been tested. The system automatically searches and tracks, in 3D, multiple retro-targets attached to an object. Stability of the photo-solution is equivalent to the results obtained using existing video cameras but with the added feature of generating robust pose solutions in the presence of strong background illumination. With this success, Neptec Design Group and the NRCC, in collaboration with the Canadian Space Agency, built a space-qualified version of the laser scanner prototype, that was flown in the payload bay of the shuttle Discovery during mission STS-105 (English et al., 2002). Obviously, compatibility with current B/W targets and the processing unit are key aspects in order to adopt a laser scanner system solution on-board the space shuttle. The combined solution can operate in triangulation-based mode from short to medium distance (<5 m) and photogrammetry-based mode (spatial resection). An advantage of the laser scanner is that it can also operate in imaging mode to produce dense 3D images of objects for inspection and maintenance. For longer range (above 30 m), the optical design can accommodate a TOF unit for improved photo-solution.

The system works as follows. The coordinates (X, Y, Z) from the laser scanner are transformed to pseudo-angular values i.e., ratios X/Z and Y/Z where Z is the range. These new photo coordinates are fed to the processing unit as if they were coming from a video camera. This insures compatibility with the on-board SVS. The main reason why the triangulation-based laser scanner achieves impressive results for pose computations even at medium range distances is that the ratiometric computation almost completely removes the dependencies on the laser spot position uncertainty (see Eqn. 1). An improvement close to an order of magnitude was obtained compared to computing the pose with the standard (X, Y, Z) coordinates. Details can be found in (Blais et al., 2000).

6. DISCUSSION: ABOUT STANDARDIZED TESTING

The issue of standardized testing is very important but at the same time a sensitive one. Surely, no manufacturer of 3D scanners (laser or not), modelling and inspection software tools wants to be seen in category with a bad connotation. Industry, academia and user groups will have to find a way to generate these standardized tests in order to create user confidence and market acceptance in using for instance laser scanning alone or in combination with other techniques. Barber et al. 2001 discuss current state of laser scanning, associated practical issues, the need to test in standardized way laser scanners, data processing and integration with other sources of information. Though photogrammetry is seen as a mature technology, let us not forget that the appearance on the market of high quality non-metric digital cameras made with CCD and CMOS sensors pose their own set of challenges in terms of resolution, accuracy and reliability (important topic at many ISPRS sponsored conferences).

7. CONCLUSIONS

This paper addressed the topic of integration of laser scanning and close-range photogrammetry from a multi-sensor and information fusion point of view. The literature surveyed though not exhaustive shows the interest in this topic from different research communities. A summary of the basic theory and best practices associated with laser range scanners, digital photogrammetry, processing, modelling were reviewed. We emphasized laser scanning because one specific laser scanner can't be used for volumes of different sizes and therefore, performance aspects of the different laser scanning solutions must be understood. One of the critical aspects of sensor fusion is to deal and manage the uncertainties link to the sensing devices, the environment and *a priori* information (e.g. a particular user). To justify the increased cost and complexity of a multi-sensor solution, one has to minimize the impact of those uncertainties in order to get the most out of the multi-sensor platform. Two categories of applications were covered, i.e., information augmentation and uncertainty management.

Three-dimensional laser scanning, like many new technologies in the past where novelty is often enough to attract interest, has been used in many projects as a way to produce models for visualization only. As the novelty effect diminishes, more people are looking at using that technology in practical applications and exploring new business models. This is a natural trend as a new technology, like laser scanning, shifts from its early developers and users towards mainstream users and services providers. This latter group can benefit from the knowledge generated in all the projects initiated in the last 20 years, e.g. scanners and software developments but also what works and what doesn't. In this process, sensor fusion becomes important as this relatively recent technology is integrated with more mature ones, like photogrammetry, CAD, etc.

ACKNOWLEDGEMENTS

The author wants to acknowledge the various collaborators that have participated in the results discussed in this paper: F. Blais, L. Cournoyer, S.F. El-Hakim M. Picard, M. Rioux from the

NRC Canada, G. Guidi from the University of Florence, L. Gonzo, S. Girardi from IRST, Trento and V. Valzano, A. Bandiera from the University of Lecce, Italy.

REFERENCES

Amann, M-C, Bosch, T., Lescure, M., Myllylä, R., Rioux, M., 2001. Laser ranging: a critical review of usual techniques for distance measurement. *Opt. Eng.* 40(1), pp.10-19.

Atkinson, K.B., 1996. *Close range photogrammetry and machine vision*. Cathness, U.K., Whittles.

Baribeau, R., Rioux, M., 1991. Influence of Speckle on Laser Range Finders. *Appl. Opt.*, 30, pp. 2873-2878.

Baltsavias, E.P., 1999a. A comparison between photogrammetry and laser scanning. *ISPRS Journal of Photogrammetry & Remote Sensing,* 54, pp. 83–94.

Baltsavias, E.P., 1999b. Airborne laser scanning: basic relations and formulas. *ISPRS Journal of Photogrammetry & Remote Sensing,* 54, pp. 199–214.

Barber, D., Mills, J., Bryan, P.G., 2001. Laser Scanning and Photogrammetry-21th Century Metrology. In: *CIPA 2001 Intern. Symp., Surveying and Documentation of Historic Buildings, Monuments, Sites*, Potsdam, Germany.

Beraldin, J.-A., Rioux, M., Blais, F., Couvillon, R.A., 1994. Digital three-dimensional imaging in the infrared at the National Research Council of Canada. In: *SPIE Proc., Intern. Symp. on Optics, Imaging, and Instrum.: Infrared Techn. XX, Session,* San Diego, CA. July 24-29, Vol. 2269, pp. 208-225.

Beraldin, J.-A., Cournoyer, L., Rioux, M., Blais, F., El-Hakim, S.F., Godin, G., 1997. Object model creation from multiple range images: acquisition, calibration, model building and verification. In: *First Intern. Conf. on Recent Advances in 3-D Digital Imaging and Modeling,* Ottawa, Ont. May 12-15, pp. 326-333.

Beraldin, J.-A., Blais, F., Rioux, M., Domey, J., Gonzo, L., De Nisi, F., Comper, F., Stoppa, D., Gottardi, M., Simoni, A., 2003. Optimized position sensors for flying-spot active triangulation systems. In: *Fourth Intern. Conf. on 3-D Digital Imaging and Modeling*, Banff, Canada, 6-10 Oct., pp. 29 – 36.

Blais, F., Rioux, M., 1986. Real-time numerical peak detector. *Signal Processing*, 11(2), pp. 145-155.

Blais, F., Beraldin, J.-A., El-Hakim, S., 2000. Range error analysis of an integrated time-of-flight, triangulation, and photogrammetric 3D laser scanning system. In: *Laser Radar Technology and Applications V,* SPIE Vol. 4035*,* Orlando, FL, April 24-28. pp. 236-247.

Blais, F., 2004. A review of 20 years of range sensor development. *Journal of Elect. Imaging.* 13(1), pp. 231-243.

Boehler, W., Bordas Vicent, M., Marbs, A., 2003. Investigating laser scanner accuracy. In: *XIXth CIPA Symposium*, Antalya, Turkey, 30 Sept. – 4 Oct.

Buzinski, M., Levine, A., Stevenson, W.H., 1992. Performance characteristics of range sensors utilizing optical triangulation. In: *IEEE 1992 National Aerospace and Electronics Conference,* pp. 1230-1236.

Callieri, M., Cignoni, P., Ganovelli, F., Impoco, G., Montani, C., Pingi, P., Ponchio, F., Scopigno, R., 2004. Visualization and 3D Data Processing in the David Restoration, *IEEE Computer Graphics and Applications*, March/April, pp-16-21.

CIPA Working Group 6 & ISPRS Commission V. 2002. Corfu, Greece, Sept. 1-2.

Colet, P., 2003. Imaging system measures space vehicle surfaces. *Advanced Imaging magazine*. pp. 18.

Dorsch, R.G., Hausler, G., Herrmann, J.M., 1994. Laser triangulation: fundamental uncertainty in distance measurement. *Appl. Opt.* 33, 1306–1314.

El-Hakim, S.F., Beraldin, J.-A., 1994. On the integration of range and intensity data to improve vision-based three-dimensional measurements. In: *Videometrics III*, Boston, MA. 2-4 Nov., SPIE Vol. 2350, pp. 306-321.

El-Hakim, S.F., Beraldin, J.-A., Blais, F., 1995. A Comparative Evaluation of Passive and Active 3-D Vision Systems. In: *Digital Photogrammetry and Remote Sensing '95*,St-Petersburg, June 25-30, SPIE Vol. 2646, pp. 14-25.

El-Hakim, S. F., 2001. Three-dimensional modeling of complex environments. In: *Videometrics and Optical Methods for three-dimensional Shape Measurement*, San Jose, Jan 20-26, SPIE Vol. 4309, pp. 162-173.

El-Hakim, S.F., Beraldin, J.-A., Blais, F., 2003. Critical factors and configurations for practical image-based 3D modeling. In: *6th Conference on 3D Measurement Techniques*. Zurich, Switzerland. Sept. 22-25, Vol. II, pp. 159-167.

El-Hakim, S.F., Beraldin, J.-A., Picard, M., Vettore, A., 2003. Effective 3D modeling of heritage sites. In: *Fourth Intern. Conf. on 3-D Digital Imaging and Modeling*, 6-10 Oct. Banff, Canada, pp. 302 – 309.

English, C.E., Samson, C., Christie, I., Blais, F., Cournoyer, L., Picard, M., 2002. Production of Models of the International Space Station Elements from 3D Laser Images. In: *Optoelectr., Photonics, and Imaging (Opto Canada 2002)*, Ottawa, Canada. May 9-10, http://iit-iti.nrc-cnrc.gc.ca/publications/nrc-44922_e.html

Fisher, R.B., Naidu, D.K., Singhal, D., 1993. Rejection of spurious reflections in structured illumination range finders. In: *2nd Conference on Optical 3D Measurement Techniques*, Zurich, Switzerland, pp. 467-474.

Fraser, C.S, 1987. Limiting error propagation in network design. *Photogrammetric Engineering and Remote Sensing*, 53(5), pp. 487-493.

Forstner, W, 1994. Diagnostics and performance evaluation in computer vision. In: *NSF/ARPA Workshop: Performance versus Methodology in Computer Vision*, pp. 11-25.

Godin, G., Rioux, M., Beraldin, J.-A., Levoy, M., Cournoyer, L., Blais, F., 2001. An assessment of laser range measurement on marble surfaces. In: *5th Conference on Optical 3D Measurement Techniques*, Wien, Austria, Oct. 1-4, pp. 49-56.

Guidi, G., Beraldin, J.-A., Atzeni C., 2004. High-Accuracy 3-D Modeling of Cultural Heritage: The Digitizing of Donatello's "Maddalena". *IEEE Trans, on Image Proc.*, 13(3), pp. 370-380.

Gruen A., Remondino F., Zhang L., 2003. Computer Reconstruction and Modeling of t he Great Buddha of Bamiyan, Afghanistan. In: *19th CIPA International Symposium*, Antalya, Turkey, pp. 440-445.

Hall, D.L., Llinas, J., 1997. An Introduction to Multisensor Data Fusion. *Proceedings of the IEEE*, 85(1), pp. 6-23.

Hebert, M., Krotkov, E., 1992. 3-D Measurements from Imaging Laser Radars: How Good Are They? *International Journal of Image and Vision Computing*, 10(3), pp. 170-178.

Hong, L., 1999. Sense your world better: multisensor/information fusion. *IEEE Circuits and Systems Newsletter*, 10(3), pp. 7-28.

Jähne, B., Haußecker, H., Geißler, P., 1999. Handbook of Computer Vision and Applications. Academic Press, San Diego.

Johansson, M., 2002. Exploration into the behaviour of three different high-resolution ground-based laser scanners in the built environment. In: *Workshop on Scanning for Cultural Heritage Recording – Complementing or Replacing Photogrammetry*, Corfu, Greece, Sept. 1-2, pp. 33-38.

Johnson, A. E., Manduchi, R. 2002. Probabilistic 3D fusion for adaptive resolution surface generation. In: *IEEE Proc. of the Intern. Symposium on 3D Data Processing Visualization and Transmission*, Padova, Italy. June 19-21, pp. 578-587.

Johnson, A. E., Kang, S.B., 1997. Registration and integration of textured 3D data. In: *First Intern. Conf. on Recent Advances in 3-D Digital Imaging and Modeling,* Ottawa, Ont. May 12-15, pp. 234-241.

Jokinen, O., Haggrén H., 1998. Statistical analysis of two 3-D registration and modeling strategies. *ISPRS Journal of Photogrammetry & Remote Sensing*, 53, pp. 320–341.

Koskinen, M., Kostamovaara, J., Myllylä, R., 1991. Comparison of the continuous wave and pulsed time-of-flight laser rangefinding techniques. In: *Optics, Illum., and Image Sensing for Machine Vision VI,* SPIE Vol. 1614, pp.296-305.

Laboureux, X., Häusler, G., 2001. Localization and registration of three-dimensional objects in space—where are the limits? *Applied Optics*, 40(29), pp. 5206-5216.

Llinas, J., Waltz, E., 1990. *Multisensor Data Fusion*. Boston, MA, Artech House.

Naidu, K., Fisher, R. B., 1991. A Comparative Analysis of Algorithms for Determining the Peak Position of a Stripe to Sub-pixel Accuracy. In: *British Machine Vision Association Conference*, Glasgow. Springer-Verlag, London, pp. 217-225.

Nitzan, D., 1988. Three-dimensional vision structure for robot applications. *IEEE Transactions on Pattern Analysis and Machine Intelligence*, 10(3), pp. 291-309.

Okatani, I.S., Deguchi, K., 2002. A method for fine registration of multiple view range images considering the measurement error properties. *Computer Vision and Image Understanding*, 87, pp. 66-77.

Paakkari, J. Moring, I., 1992. Method for evaluating the performance of range imaging devices. In: *Industrial Applications of Optical Inspection, Metrology, and Sensing*, SPIE Vol. 1821, pp. 350-356.

Poor, H.V., 1994. An introduction to signal detection and estimation. 2nd Ed., *Springer-Verlag, NY.* Chap VII. p. 331.

Rioux, M., 1984. Laser Range Finder based on Synchronized Scanners. *Appl. Opt.*, 23, pp. 3837-3844.

Rioux, M., Bechthold, G., Taylor, D., Duggan, M., 1987. Design of a large depth of view three-dimensional camera for robot vision. *Opt.Eng.* 26(12), pp. 1245–1250.

Rioux, M., 1994. Colour 3-D electronic imaging of the surface of the human body. In: *Automatic Systems for the Identification and Inspection of Humans*, San Diego, CA. July 28-29, 1994. SPIE Vol. 2277, pp. 42-54.

Scaioni, M., Vassena, G., Kludas, T., Pfeil, J.-U., 1996. Automatic DEM generation using digital system induscan. In: *Int. Arch. Photogram. Remote Sensing*, Vienna, Austria, Vol. XXXI, pp. 581–586.

Schneider, R., Thürmel, P., Stockmann, M., 2001. Distance measurement of moving objects by frequency modulated laser radar. *Opt. Eng.* 40. pp. 33-37.

Soucy, M., Laurendeau, D., Poussart, D., Auclair, F., 1990. Behaviour of the center of gravity of a reflected gaussian laser spot near a surface reflectance discontinuity. *Industrial Metrology*, 1(3), pp.261-274.

Soucy, M. Godin, G. Baribeau, R. Blais, F. and Rioux, M., 1996. Sensors and algorithms for the construction of digital 3-D colour models of real objects. In: *Proc. of the IEEE ICIP*, Lausanne, Suisse. Sept. 16-19, Vol. II, pp. 409-412.

Velios, A., Harrison, J.P., 2002. Laser scanning and digital close range photogrammetry for capturing 3D archaeological objects: a comparison of quality and practicality. In: *G. Burenhult (ed.), Archaeological Informatics: Pushing the Envelope, CAA 2001*, Oxford, pp. 205-211.

VIM, 1993. *ISO International Vocabulary of Basic & General Terms in Metrology.* 2nd Edition, International Organization for Standardization, Geneva.

VDI/VDE 2634 Blatt 2, 2002. *Optische 3D-Messsysteme – Systeme mit flächenhafter Antastung/Optical 3-D measuring systems - Optical systems based on area scanning.*

Wallace, A.M., Liang, B., Trucco, E., Clark, J, 1999. Improving depth image acquisition using polarized light. *Intern. Journal of Computer Vision*, 32(2), pp. 87-109.

Wendt, A., Rosing, C., Weisensee, M., 2002. Comparison of different sensor types and validation of an approach for multi sensor fusion. In: *Close-Range Imaging, Long-Range Vision. Commission V*, XXXIV, Part 5, 2-6 Sept., Corfu, pp. 105-109.

Wehr, A., Lohr, U., 1999. Airborne laser scanning – an introduction and overview. *ISPRS Journal of Photogrammetry & Remote Sensing*, 54, pp. 68-82.